# Antimicrobial effects of free nitrous acid on *Desulfovibrio vulgaris*: implications for sulfide induced concrete corrosion

Shu-Hong Gao[1], Jun Yuan Ho[1], Lu Fan[1,2], David J Richardson[3], Zhiguo Yuan[1] and Philip L Bond[1]*

[1]Advanced Water Management Centre, The University of Queensland, St. Lucia, Brisbane, QLD 4072, Australia

[2] iCarbonX, Shenzhen 518053, China

[3] University of East Anglia, Norwich Research Park, Norwich, NR4 7TJ

**Running title:** Inhibitory mechanisms of FNA on *D. vulgaris*

*Corresponding author

Philip L Bond, Level 4 Gehrmann Building, Advanced Water Management Centre, The University of Queensland, St. Lucia, Brisbane, QLD 4072, Australia

Phone: + 61 7 3346 3226

FAX: + 61 7 3365 4726

E-mail: phil.bond@awmc.uq.edu.au

## Abstract

Hydrogen sulfide produced by sulfate reducing bacteria (SRB) in sewers causes odor problems and asset deterioration due to the sulfide induced concrete corrosion. Free nitrous acid (FNA) was recently demonstrated as a promising antimicrobial agent to alleviate hydrogen sulfide production in sewers. However, knowledge of the antimicrobial mechanisms of FNA is largely unknown. Here we report the multiple-

targeted antimicrobial effects of FNA on the SRB *Desulfovibrio vulgaris* Hildenborough by determining growth, physiological and gene expression responses to FNA exposure. The activities of growth, respiration and ATP generation were inhibited when exposed to FNA. These changes were reflected in transcript levels detected during exposure. Removal of FNA was evident by nitrite reduction that likely involved nitrite reductase and the poorly characterised hybrid cluster protein, and the genes coding for these proteins were highly expressed. During FNA exposure lowered ribosome activity and protein production were detected. Additionally, conditions within the cells were more oxidising and there was evidence of oxidative stress. Based on interpretation of the measured responses we present a model depicting the antimicrobial effects of FNA on *D. vulgaris*. These findings provide new insight for understanding the responses of *D. vulgaris* to FNA and will provide foundation for optimal application of this antimicrobial agent for improved control of sewer corrosion and odor management.

Keywords: free nitrous acid; antimicrobial agent; inhibitory mechanism; *Desulfovibrio vulgaris* Hildenborough

## Importance

Hydrogen sulfide produced by SRB in sewers causes odor problems and results in serious deterioration of sewer assets that requires very costly and demanding rehabilitation. Currently, there is successful application of the antimicrobial agent free nitrous acid (FNA), the protonated form of nitrite, for the control of sulfide levels in sewers (1). However, the details of the antimicrobial mechanisms of FNA are largely unknown. In this study, we identified the key determinants (inhibiting anaerobic

respiration, reducing FNA, causing oxidative stress, and shutting down protein synthesis) for how *Desulfobivrio vulgaris* Hildenborough, a model sewer corrosion bacterium, responds to FNA by examining the growth, physiological and gene expression changes. These findings provide new insight and underpinning knowledge for understanding the responses of *D. vulgaris* to FNA exposure, thereby benefiting the practical application for improved control of sewer corrosion and odor.

## Introduction

Sulfate reducing bacteria (SRB) are anaerobic chemoorganotrophic microorganisms that typically use sulfate as the terminal electron acceptor for respiration and generate energy with the production of hydrogen sulfide (2). In confined spaces production of hydrogen sulfide can cause odor and corrosion problems. This is particularly the case in sewers and inlet structures of wastewater treatment plants where the oxidation of sulfide produces sulfuric acid which corrodes the concrete surfaces of the sewer. This results in serious deterioration of sewer assets that requires very costly and demanding rehabilitation efforts (3, 4). Consequently there is great interest to efficiently control SRB and thereby minimising hydrogen sulfide production in sewers.

Various chemical dosing methods are used to lower hydrogen sulfide production in sewers and four strategies currently used include: sulfide oxidation by injection of chemical oxidants such as air, oxygen, or nitrate (5, 6); sulfide precipitation by addition of iron salts (7); application of magnesium hydroxide or lime to raise the wastewater pH and prevent the release of hydrogen sulfide (8); and to inhibit the activities of SRB to lessen the generation of hydrogen sulfide (9). However, to obtain

the required sulfide control these strategies require continuous chemical consumption and considerable operational costs (10).

Free nitrous acid (FNA), the protonated form of nitrite, was recently demonstrated to be the true metabolic inhibitor behind the usually observed “nitrite inhibition” (11). In recent treatment of sewer biofilms it was seen that application of FNA for 6-24 hours at 0.2-0.3 mg N/L decreased the live cell percentage from about 80% to 5-15% (3). Since then FNA has been applied in sewer field trials in which an 80% reduction of sulfide production was achieved by intermittent FNA dosing at 0.26 mg N/L for 8-24 hours every four weeks (1). These investigations support that the application of FNA for control of sulfide levels in sewers is highly feasible.

Therefore, FNA is emerging as an extremely promising antimicrobial agent for the control of SRB, their activities and sulfide production, and there is great interest to understand how SRB respond to and withstand exposure to FNA. Nitrite is reported to cause decreased expression of the genes coding for dissimilatory sulfite reductase (DsrAB) and thereby disrupting respiration of SRB (12, 13). Currently, the antimicrobial effects of FNA on bacteria in general are believed to be multi-targeted (14). It is thought that FNA, and perhaps reactive nitrogen species (RNS) derived from FNA, causes oxidative stress resulting in damage to cell enzymes, cellular membranes and walls, and nucleic acids (15). Other hypotheses to explain the antimicrobial effects include FNA causing disruption of the proton motive force (16), nitrosylation of metal centres or thiol groups in enzymes (17), and DNA mutation (14). However, these hypotheses are not well verified and it is not clear whether some of

these effects are more important than others in different bacteria. Additionally, different bacteria will have different levels of tolerance to FNA (18).

*Desulfovibrio* species can be prevalent SRB in sewers (19) and are likely important for hydrogen sulfide production in sewage. *Desulfovibrio vulgaris* Hildenborough is well studied and is demonstrated to have a periplasmic cytochrome c nitrite reductase (NrfA) for the conversion of nitrite to ammonium (2). It is largely thought that this nitrite reductase activity is not respiratory or for growth (20), but is a mechanism to remove the toxic nitrite (13). Although, in a recent twist there is suggestion that the nitrite reduction activity can conserve energy for growth (21).

To date, there have been some transcriptional investigations, based on macroarray and microarray analyses, to examine the effects of nitrite on *D. vulgaris* (12, 13) . These studies implicate that nitrite stress could inhibit sulfate reduction and cause possible oxidative stress, as well as disrupt iron homeostasis. However, all the conclusions and hypotheses drawn from those investigations are based only on the transcriptional responses. A comprehensive and systematic understanding of the antimicrobial mechanisms of FNA on *D. vulgaris* is still lacking. This could be achieved by combining the transcriptional response with detection of cell activities and physiological changes.

In this study, substrate transformations and physiological changes were detected in response to different levels of FNA. In addition, whole genome messenger RNA sequencing (RNA-seq) analysis was also conducted on *D. vuglaris* cultures in the presence and absence of sub-bactericidal level of FNA (4.0 μg N/L). The global

transcriptome response was combined with analyses of substrate transformations and physiological responses to test the hypotheses mentioned above. From this a more comprehensive understanding of the effects of FNA was obtained to verify the key determinants of FNA stress in this model sewer hydrogen sulfide producing bacterium.

## Material and Methods

### Cultivation of *D. vulgaris* Hildenborough

*D. vulgaris* Hildenborough (ATCC 29579) was provided by Professor Jizhong Zhou and Dr. Aifen Zhou from Institute for Environmental Genomics, University of Oklahoma. For all experiments, a defined lactate sulfate medium (LS4D medium) (22) was used to cultivate the bacterium. The LS4D medium was prepared and added to serum bottles, gassed with nitrogen gas for 30 min before capping with butyl rubber stoppers for autoclaving. 1.5 ml of a glycerol preserved stock of *D. vulgaris* was used to inoculate the serum bottles containing 140 ml of medium. These were then cultivated at 37°C for 48 h to achieve the early stationary phase of growth (an optical density at 600 nm [$OD_{600}$] of 0.9 to 1.0). The $OD_{600}$ of the culture was then adjusted to 0.5 and multiple 10 ml aliquots of this was used to inoculate serum bottles containing 140 ml of fresh LS4D medium. The inoculated bottles were then incubated at 30°C without shaking for further use of experiments described below. All experimental procedures of culture growth, physiological assays and RNA-seq analyses were performed on triplicate cultures unless otherwise mentioned.

### FNA treatment on cultures of *D. vulgaris*

After 26 h growth at 30°C, when the cultures were in early log phase ($OD_{600}$ of around 0.3), nitrite was added to achieve the starting FNA concentrations of 0, 1.0,

149 4.0, and 8.0 μg N/L. The term "starting concentration" is used to describe the levels of
150 FNA added in the different experiments, as during the incubations the actual FNA
151 concentrations change, most likely due to the nitrite reduction activity of *D. vulgaris*.
152 For each FNA concentration the culture incubations were performed in triplicate. The
153 FNA concentration is dependent on the level of nitrite, pH and temperature, and this
154 was calculated based on the equation already described (23). These concentrations of
155 FNA were chosen based on preliminary studies (not shown) where it was observed
156 that these levels of exposure covered the spectrum of growth responses to FNA, from
157 slight inhibition of growth to near complete killing of the organism. Following the
158 addition of FNA the cultures were incubated for a further 48 h at 30°C. During
159 exposure to the different FNA levels the concentrations of lactate, acetate, sulfate,
160 sulfite, sulfide, thiosulfate, nitrite and FNA were determined from filtered samples of
161 the inoculated cultures. Additionally, samples from the triplicate controls (no added
162 FNA) and FNA-treated cultures (4.0 μg N/L) were taken for RNA extraction at 1 h
163 after FNA addition. These conditions were chosen for study of the transcriptional
164 response as (i) it has been previously observed in *D. vulgaris* that the peak of the gene
165 expression response to nitrite occurs at 1 h after nitrite exposure (13), and (ii) our
166 preliminary studies showed that at 4.0 μg N/L of FNA exposure there was significant
167 effect on the organisms growth, but complete killing did not occur and eventually the
168 organism could overcome the stress. In preparation for the RNA extraction 5 ml of the
169 bacterial suspension from each serum bottle was centrifuged at 13,000 x g for 2
170 minutes, the supernatant was discarded and the pellets were immediately frozen in
171 liquid nitrogen before storing at -80ºC. Total RNA extraction was performed from the
172 pellets using the QIAGEN miRNeasy Mini Kit (catalog number 217004) according to
173 the manufacturer's instructions, except for the addition of an extra bead-beating step

to ensure the complete lysis of the cells. Strand-specific cDNA libraries were constructed and Illumina paired-end sequencing (HiSeq 2000, Illumina Inc., San Diego, CA, USA) was performed (Macrogen, Seoul, Korea) on the extracted RNA. The raw sequencing data was deposited in NCBI's Gene Expression Omnibus and are accessible through GEO series accession number GSE78834.

**Chemical analyses of culture samples**

Culture $OD_{600}$ and pH were monitored during the incubations with a Cary 50 bio UV visible spectrophotometer (Varian, Australia) and a labCHEM-pH Benchtop pH - mV - Temperature Meter, respectively. Slight increases in pH occurred during incubation which ranged from 7.15 to 7.4 due to the conversion of nitrite to ammonium. For nitrite detection, culture samples were taken, immediately filtered through 0.22 µm filters (Merck Millipore, USA) and analysed on a Lachat QuikChem 8000 flow injection analyzer (FIA). The concentrations of sulfur species (sulfide, sulfite, thiosulfate, and sulfate) were determined in culture samples by ion chromatography. For this 1.5 ml samples were filtered (0.22 µm, Merck Millipore, USA) into 2 ml vials that contained 0.5 ml of an anti-oxidant preservative buffer (24). Samples were then analysed within 24 h by ion chromatography (Dionex ICS-2000). The culture lactate and acetate levels were determined in 1.0 ml filtered (0.22 µm, Merck Millipore, USA) samples by high performance liquid chromatography as previously described (25).

**Physiological assay of *D. vulgaris***

Various assays were conducted during growth of *D. vulgaris* in the absence and presence of different FNA concentrations. LIVE/DEAD staining was conducted on the culture samples as described in the manufacturers instructions (BacLight Bacterial

Viability Kit, Molecular Probes, L7012). The LIVE/DEAD ratio of cells was then quantified by applying 500 µL of the stained samples to a FACSAria™ II (BD Biosciences, San Jose, USA) flow cytometer. The cellular redox status of the cultures was determined by staining 500 µL of samples with the RedoxSensor™ Green reagent provided in the BacLight RedoxSensor Green Vitality Kit (Life Technologies, B34954), as per the manufacturers instructions. The fluorescence signal of the stained cultures was quantified using the FACSAria™ II type flow cytometer as suggested in the kit protocol. Cellular ATP levels were determined in 500 µL of culture samples using the BacTiter-Glo™ Microbial Cell Viability Assay (Promega Corporation, G8231). Cellular thiol group levels were determined on 200 µL culture samples using the Thiol and Sulfide Quantitation Kit (Molecular Probes, T-6060). The ATP and thiol group assays were performed as described in the corresponding manufacturers instructions.

**RNA-seq data processing and differentially expressed genes analysis**

The raw sequence reads were treated using the NGS QC Toolkit (v2.3.3) (26) to trim the 3'-end residual adaptors and primers as well as removing the ambiguous characters in the reads. Then the sequence reads consisting of at least 85% bases with a quality value ≥ 20 were kept. The resulting clean reads no shorter than 75 base pairs were used for downstream analyses. SeqAlto (version 0.5) was used to align the clean reads of each sample to the reference genome (NC_002937) of *D. vulgaris* (27). Cufflinks (version 2.2.1) was used to calculate the strand-specific coverage for each gene and to analyse the differential expression on triplicated cultures (28). CummeRbund package in R (http://compbio.mit.edu/cummeRbund/) was used to conduct the statistic analyses and visualization. Gene expression was calculated as

reads per kilobase of a gene per million mapped reads (RPKM), a normalized value generated from the frequency of detection and the length of a given gene (28). Differences in fold-change values were calculated between control and FNA-treated samples (4.0 μg N/L) by determining the $\log_2$ fold-change (LFC) of the averaged RPKM values of two triplicated experiments. A stringency cut-off of LFC $\geq 1$ or $\leq -1$ with q value less than 0.05 was used to identify the significantly differentially expressed genes.

## Results

### Concentration-dependent effects of FNA on culture growth and respiratory activities

In these investigations, *D. vulgaris* utilises sulfate as the electron acceptor and lactate as the electron donor with sulfide and acetate as the respective end products (2). Additionally, *D. vulgaris* has NrfA that can reduce nitrite to ammonium, allowing it to survive in environments in the presence of nitrite (2). The growth of *D. vulgaris* cultures exposed to the lowest starting FNA concentration of 1.0 μg N/L was slightly inhibited during the 48 h incubation (Figure 1). Inhibition of growth increased with the increasing levels of FNA and growth was almost completely stopped with FNA at 8.0 μg N/L (Figure 1).

In the presence of FNA at 1.0 μg N/L the levels of lactate oxidation and sulfate reduction were slightly less than that of the control culture (no FNA addition) (Figure 2C, E) and this coincided with the observed slight decreased growth (Figure 1), indicating FNA was having only a slight inhibitory effect on the organism at this level. During the incubation 1.0 μg N/L FNA was completely reduced within 8 h after

addition (Figure 2A, B). In comparison, much lower lactate oxidation levels were detected in cultures with starting FNA concentrations of 4.0 and 8.0 μg N/L (Figure C). In these cultures there would be limited electrons available for sulfate reduction, which was severely diminished (Figure 2E), and this coincided with the reductions in growth levels detected (Figure 1). In the batch cultures nitrite reduction occurred (Figure 2 A, B) after FNA addition. This was evident at all FNA concentrations and was likely due to nitrite reductase activity of *D. vulgaris*.

The absolute ratios of lactate consumed, sulfate used and acetate produced were calculated from the concentrations detected during the 48 h incubations of *D. vulgarius* at the different FNA levels. The ratios were compared to the theoretical ratio determined when acetate is considered as the product of the lactate oxidation (Table 1). For the control culture not exposed to FNA, these values are reasonably close to the stoichiometric ratios for the lactate oxidation (Table 1). However, the ratios of lactate used and acetate produced were increased, at the higher level of applied FNA. This could be explained if there was increased competition for electrons during FNA exposure, which may likely have resulted from increased nitrite reduction activity.

Sulfite and thiosulfate levels were detected during the batch incubations (Figure 2G, H). There were no obvious differences in the levels of sulfite that correlated with the different FNA levels while thiosulfate was detected only in the cultures that were exposed to FNA levels of 4 and 8 μg N/L (Figure 2H).

**Changes in specific cell activities during FNA exposure**

LIVE/DEAD staining was performed on the *D. vulgaris* batch cultures to evaluate the effect of FNA on cell viability. At early log phase prior to FNA addition, the viable cell numbers in the cultures were around 85%-90% (Figure 3A). When no FNA was added, the live cell percentage stayed at this level until 24 h incubation before dropping to around 65% at 48 h incubation (Figure 3A). This drop in live cells could have resulted from changes in the culture conditions, such as lactate depletion (Figure 2C). In comparison, the viable cell numbers for the FNA concentration of 1.0 μg N/L decreased quickly to around 60% when the incubation time was 7 h and this remained near that level through the incubation period (Figure 3A). Substantial decreases in the percentage of live cells were detected immediately upon the addition of FNA at 4.0 μg N/L FNA, and at 8.0 μg N/L, such that near 95% killing of the *D. vulgairs* cultures occurred within 12 h incubation (Figure 3A). These results support the suggestion that the bacteriostatic and bactericidal effects of FNA are concentration-determined and population-specific as previously detected in *Pseudomonas aeruginosa* PAO1 (23).

Cellular thiol levels of *D. vulgaris* increased with the addition of FNA (Figure 3B). At FNA starting concentrations of 1.0 and 4.0 μg N/L N/L, a small increase in cellular thiol levels was detected at 12 and 24 h incubation (Figure 3B). However, cellular thiol levels increased markedly throughout the incubation period when the cells were exposed to 8.0 μg N/L FNA (Figure 3B). It is thought that FNA could nitrosylate thiol groups, such as those on proteins, which could change the activity or function of those (14). There is also hypothesis that FNA imposes oxidative stress on bacteria cells (29). Thus in these batch cultures the cell redox status was determined and it was observed that with increasing levels of FNA the cells were more oxidised (Figure 3C). Cellular ATP levels of the *D. vulgaris* batch cultures (normalised to per live cell) decreased

with the increase of added FNA concentrations (Figure 3D). This supports the idea that FNA acts as a protonophore, to decouple the proton motive force across cell membranes and thereby inhibiting ATP synthesis (16).

**Global transcriptomic analysis of FNA stress**

To determine the antimicrobial mechanisms of FNA and the possible response pathways adopted by *D. vulgaris*, gene expression profiles were examined by RNA sequencing. To focus on the direct inhibitory mechanisms of FNA on *D. vulgaris* we sought to measure changes that report on the primary effect of FNA, not any secondary affects that would occur over longer timescales more related to changes in growth rate, substrate, products and batch conditions, rather than the direct response to FNA. We therefore measured the transcriptional response after only 1 h of the FNA addition. This was performed when the cultures were exposed to 4.0 μg N/L at 1 h after FNA addition and compared to gene expression of control cultures when no FNA was added. A total of 239 genes, 6.6% of the total 3623 genes, were detected as significantly differently expressed (see criterion in Material and Methods). 159 genes showed increased transcripts and 80 genes showed decreased transcript levels in response to FNA stress.

**Evidence of oxidative stress and detoxification of FNA by *D. vulgaris***

*D. vulgaris* possesses NrfA that can catalyse the six-electron reduction of nitrite to ammonium and hydroxylamine is an intermediate of the reduction (30). In these FNA-added cultures the gene coding for NrfA (DVU0625) exhibited considerable up regulation (Table 2), implying its detoxifying role by the reduction of nitrite (and proportional reduction of FNA). This observation agrees with the decreasing nitrite

levels detected in the batch cultures (Figure 2A). Additionally, the gene, DVU2543, which codes for what is known as the hybrid cluster protein (HCP), was the most up-regulated gene detected when exposed to FNA (Table 2). The HCP is proposed to have hydroxylamine reductase activity (31), and was possibly acting to remove hydroxylamine as part of the detoxification of nitrite.

Various genes coding for response to oxidative stress displayed highly increased transcript levels in the FNA-added cultures (e.g. DVU0772 and *ahpC* (DVU2247), Table 2). This implies that FNA caused oxidising conditions, which is what was detected by the cellular redox measurement in FNA-added cultures (Figure 3C). The genes *msrA* (DVU1984) and *msrB* (DVU0576), coding for reductases, that reduce methionine sulfoxides as an antioxidant response, were observed to have increased transcript levels in FNA-added cultures. Additionally, genes of the Fur regulon, DVU0273, *gdp* (DVU3176), and DVU2574, showed increased transcript levels in response to FNA (Table 2), indicating the possibility that FNA causes a response relating to iron levels change in the cell. Alternatively, this could also a response to increased oxidative condition, as the genes involved in oxidative stress and iron homeostasis are of the same superfamily of metalloregulatory proteins (13).

**FNA inhibited anaerobic respiration and energy generation**

In the presence of FNA, various genes coding for enzymes involved in lactate oxidation and sulfate reduction processes were down regulated (Table 3). This included the genes DVU0849-50 and DVU1286-90 that code for the quinone-interacting membrane-bound oxidoreductase complex (Qmo) and the sulfite reductase complex (DsrAB) respectively (Table 3). It is proposed that Qmo transfers electrons

349 from lactate oxidation directly to adenosine-5'-phosphosulfate reductase while DsrAB
350 transfers electrons to the sulfite reductase (2).
351
352 Recently an operon has been described for lactate oxidation genes (luo) in *D. vulgaris*
353 (32). This includes the genes DVU3026 for lactate permease, DVU3027-28 and
354 DVU3032-33 for lactate dehydrogenase subunits, DVU3025 for pyruvate-ferredoxin
355 oxidoreductase, DVU3030 for acetate kinase, and DVU3029 for phosphate
356 acetyltransferase. Down-regulation of all these genes in the luo operon, excepting
357 DVU3026, was observed when exposed to FNA (Table 3). Other genes proposed for
358 lactate oxidation such as DVU0600 for lactate dehydrogenase and DVU1569-70 for
359 pyruvate-ferredoxin oxidoreductase, were up regulated or had no change respectively
360 in the presence of FNA. However, DVU0600 and DVU1569-70 had very low
361 expression values (Table 3), and as discussed later, there is some question regarding
362 the involvement of the proteins coded by these genes in lactate oxidation.
363
364 Down regulation of these genes, involved in lactate oxidation and transfer of electrons
365 for sulfate reduction, correlated with reductions of lactate and sulfate utilisation
366 (Figure 2C, E) and lowered acetate and sulfide production (Figure 2D, F) when *D.*
367 *vulgaris* was exposed to FNA. Additionally, the transcripts of genes DVU0774-80,
368 and DVU0918 coding for ATP synthase were all markedly down regulated (Table 3).
369 This coincided with the lowered ATP level detected in the cells. It seems the cells
370 were shutting down the main energy conserving reactions when exposed to FNA.
371
372 **FNA disrupts DNA replication, transcription and translation**

373 Genes encoding for critical enzymes involved in DNA replication (e.g. chromosomal
374 replication initiator protein DnaA, DNA polymerase, DNA gyrase, DNA
375 topoisomerase) and transcription (DNA-directed RNA polymerase) exhibited down
376 regulation after FNA exposure for 1 h (Table 4). As well, the genes coding for 30S
377 and 50S ribosomal structure proteins (Table 4) and a variety of amino acid transfer
378 RNA synthetases showed significantly decreased transcripts. It is apparent that FNA
379 could be causing decreased cell activities of DNA replication, transcription and
380 protein biosynthesis in *D. vulgaris*. The phenomenon of decreased DNA replication,
381 transcription and protein synthesis coincides with the decreased growth and overall
382 metabolism we detected, such as the decreased ability to utilise sulfate and lactate,
383 during FNA exposure (Figure 1 and 2). The gene *yfi* (DVU1629) coding for the
384 ribosomal subunit interface protein displayed 14.4 fold up regulation (Table 4). This
385 factor is demonstrated to stabilise ribosomes and stop translation in stressful
386 conditions (33). Possibly *D. vulgaris* is ceasing translation, and inactivates/conserves
387 the existing ribosomes in the presence of FNA. Consequently, we measured protein
388 levels per live cell of the control and FNA exposed (4.0 µg N/L) cultures after 2 and
389 8 h incubation periods (Table 5). Protein levels per cell were less in the FNA- added
390 culture in comparison to the control, suggesting that protein synthesis was markedly
391 arrested when exposed to FNA. This is in agreement with the decreased expression
392 we detected of many genes involved with ribosome function (Table 4).
393
394 Additionally, the genes coding for DNA repair proteins MutL and RadC showed
395 increased transcript levels when FNA was applied (Table 4). This was also the case
396 for genes coding for chaperone proteins DnaK and DnaJ (Table 4) that are reported to
397 assist in the re-folding of damaged proteins (34). The up regulation of these genes

indicates that FNA is likely causing damage to DNA and proteins and *D. vulgaris* was attempting the repair of these molecules.

## Discussion

In this study, the antimicrobial effects of FNA were determined in the model SRB *D. vulgaris*. For the first time we use a comprehensive approach by combining substrate consumption, physiological analyses, and whole genome RNA-seq, in the presence and absence of FNA, to discover the antimicrobial mechanisms of FNA on *D. vulgaris* Hildenborough. Our findings of the transcriptome analysis revealed significant multiple responses and detoxification activities of *D. vulgaris* in response to FNA stress, and the resulting observations and hypotheses were supported by the cell activities and physiological changes detected.

Nitrite consumption and increased transcription of genes coding for the nitrite reductase NrfA demonstrated that detoxification of FNA by NrfA was evident in *D. vulgaris* in the presence of FNA even when electron supply was low since lactate oxidation was limited (Figure 2A&C, Table 2). This is a logical response and is in agreement with previous observations of *D. vulgaris* to nitrite exposure (12, 13) . Additionally, the most up-regulated gene detected, with greater than 1000 fold change in the FNA-added cultures was DVU2543 (Table 2), which encodes a proposed hydroxylamine reductase (31). High expression of this gene in *D. vulgaris* has been reported previously in response to nitrite exposure (12, 13). The enzyme is thought to be either for reduction of RNS (the hydroxylamine reductase activity) or for reduction of reactive oxygen species (35). There is strong possibility here that hydroxylamine or other RNS accumulate during FNA exposure, possibly through incomplete reduction

423 of nitrite by NrfA (30). Characterisation of the HCP from *E. coli* shows reduction of
424 hydroxylamine with production of ammonium (31). While the enzyme has not been
425 characterised in *D. vulgaris*, one suggestion is that the HCP is acting similarly or in
426 conjunction with NrfA to detoxify the high levels of nitrite.
427
428 Genes coding for electron transfer proteins for sulfate reduction, the Qmo and DsrAB
429 membrane complexes, were significantly down regulated (Table 3). This down
430 regulated gene expression is observed in previous studies of nitrite exposure to *D.*
431 *vulgaris* (12, 13) , and would be an appropriate action in cells that experienced
432 diminished electron flow from lactate oxidation. Interestingly, thiosulfate, the
433 intermediary product of the sulfate reduction by the trithionate-reducing pathway (36),
434 was found to accumulate in FNA treated samples while sulfite did not (Fig 2G and H).
435 Previous studies demonstrate two possible pathways of sulfite reduction to sulfide in
436 *D. vulgaris*, one is by direct reduction without intermediates and the other is via the
437 trithionate pathway with thiosulfate and sulfite as the intermediates (37). The
438 observed accumulation of thiosulfate supports the inhibitory effect of nitrite on
439 DsrAB and suggests that the trithionate-reducing pathway is the mechanism of sulfite
440 reduction in *D. vulgaris* in these conditions. In summary, the FNA exposure caused
441 the down regulation of these genes which severely inhibited the lactate oxidation and
442 sulfate reduction processes.
443
444 From early annotations of the *D. vulgaris* genome the genes associated with lactate
445 oxidation have included DVU0600 for lactate dehydrogenase, and DVU1569-70 for
446 pyruvate-ferredoxin oxidoreductase. In a previous microarray study exposing *D.*
447 *vulgaris* to nitrite levels (2.5 mM) similar to that used here (2.3 mM), they reported up

448 regulation of these genes (13). We also report up regulation for the gene DVU0600
449 but no change for the genes DVU1569-70. However, the expression levels (RPKM
450 values) of these genes in the presence of FNA was extremely low (Table 3), thus, this
451 questions the involvement of the respected coded proteins in lactate oxidation.
452 Recently, genes of the luo operon are deemed to be responsible for lactate oxidation
453 in *D. vulgaris* rather than DVU0600 and DVU1569-70 (32). In this study we detected
454 down regulation of most genes in luo operon when exposed to FNA (Table 3) and
455 importantly these genes had high expression values when lactate and sulfate
456 utilisation, and when acetate and sulfide production, were active (Table 3, Figure 2C,
457 D, E, and F). This down regulation of the luo operon genes during FNA exposure is
458 logical when the cells respiratory activities were lowered, as we observed.
459 Additionally, these findings further support the involvement of the recently described
460 luo operon in lactate oxidation (32).
461
462 In addition to the down regulation of genes involved in respiration, there is suggestion
463 that FNA directly effected enzymes involved in lactate oxidation. The lack of sulfate
464 utilisation during high levels of FNA exposure can be readily explained by the
465 inhibition of the sulfite reductase activity of DsrAB by nitrite/FNA (12). However,
466 there is the question as to why the lactate oxidation stops during exposure to FNA.
467 Nitrite reductase activity in the periplasm would act to consume the protons and
468 electrons produced by lactate oxidation in the cytoplasm, as described in the model
469 for respiration by *D. vulgaris* (12). Thus, lactate oxidation should continue unless
470 FNA or nitrite was having an effect on the enzymes involved that process. The
471 periplasmic hydrogenases are involved in the flow of protons and electrons produced
472 by lactate oxidation (12). However, gene expression of the highly expressed

periplasmic hydrogenase, detected as the Ni-Fe-Se type (Table 3), was significantly decreased. Additionally, it has been seen that the activity of these hydrogenases of *D. vulgaris* is inhibited by nitrite and other RNS (38). Consequently, this lowered gene expression, and the enzyme inhibition could lower the flow of electrons and protons and explain the lowered lactate oxidation activity in the presence of FNA.

To conserve energy *D. vulgaris* performs incomplete lactate oxidation to produce acetate and uses sulfate as the electron acceptor. In our batch cultures, there is limited utilisation of lactate and sulfate, and production of acetate and sulfide at 24 h exposure of 4.0 µg N/L FNA (Figure 2). However, based on 4 electrons being released per molecule of lactate utilised, and 6 and 8 electrons required for nitrite and sulfate reductions respectively, we calculated the electron balance when the culture was exposed to FNA at 4.0 µg N/L at 48 h incubation. It was deduced that even this low amount of lactate utilisation, 7.12 mmol, would provide 28.5 mmol of electrons, which is essentially nearly enough required for the nitrite and sulfate reduction (32.5 mmol) that was detected.

During FNA exposure the cellular redox state was markedly more oxidised (Figure 3C) and genes coding for response to oxidative stress, and those involved in protein repair, had increased expression (Table 2). Additionally, as elucidated above, another possibility for the highly up-regulated gene DVU2543, is that the HCP is acting to relieve oxidative stress (35). Considering these detected events, oxidative stress is suggested as an important antimicrobial effect caused by FNA in *D. vulgaris*. While it is currently not known, it is possible that oxidative damage to the cell components was caused by RNS (14, 23). Interestingly, when P*seudomonas aeruginosa* was

498 recently exposed to FNA, a more reduced intracellular condition was caused (25).
499 Therefore, the nature of the oxidative stress caused by FNA is strain-dependent rather
500 than a general mode of action.
501
502 FNA exposure caused decreased expression of genes involved in protein synthesis in
503 *D. vulgaris*. This is consistent with previous studies of the effect of FNA on *S.*
504 *enterica* and *P. aeruginosa* (25, 39). Additionally, we detected increased expression
505 of the gene *yfi* (DVU1629) (Table 4), the coded protein of which functions to stabilise
506 ribosomes and stop translation in stressful conditions. Thus, it seems that FNA stress
507 caused *D. vulgaris* to stop protein synthesis, and to inactivate and stabilise the
508 existing ribosomes. This was supported by the decreased cellular protein levels we
509 measured during FNA exposure (Table 5). The nature of these FNA-caused changes
510 to the gene regulation detected here needs further investigation, possibly it was a
511 response to lowered cell energetics. Irrespective, the decreased ribosome activity
512 would have a major impact on the organism's ability to produce its main components
513 for successful cellular activity and operation.
514
515 Achieving control of the growth and activity of SRB in sewers is extremely important
516 to mitigate costly concrete corrosion. Growth was detected in the *D. vulgaris* batch
517 cultures at all the concentrations of FNA applied in this study (Figure 1). Although,
518 the growth was low at the high FNA starting concentration of 8.0 µg N/L, when
519 approximately 5% of cells remained live (Figure 3A). While only low levels of lactate
520 and sulfate were consumed in this condition, it appears that the remaining live cells
521 were able to grow at the high level of FNA. These results suggest that the bactericidal
522 effects of FNA are concentration-determined and higher concentrations of FNA need

523 to be applied to kill *D. vulgaris*. We recently proposed that heterogeneity in
524 P*seudomonas aeruginosa* populations explained differential resistance to FNA (23). It
525 is also possible here that differential resistance to FNA is detected in SRB. The
526 occurrence of resistance would be of concern in the application of FNA in the sewers.
527 Recently, in field trials lasting 6 months the sulfide production from actual sewer
528 biofilms was reduced by 80% after dosing the sewage with FNA at 0.26 mg N/L (1).
529 Consequently, good levels of sulfide control were achieved and increased tolerance to
530 the applied FNA was not observed under the dosing regime. Although the laboratory
531 application of FNA is very different to that in the real sewer situation, through the
532 improved understanding gained in this study, there is likely opportunity to improve on
533 real FNA applications. For example, combining FNA with treatments that cause
534 increased oxidative stress is seen to achieve more effective biofilm control (40).
535
536 In conclusion, several key findings were identified in this study regarding the
537 responses of *D. vulgaris* to FNA stress. A conceptual model was proposed that
538 summarises the antimicrobial effects of FNA on *D. vulgaris* (Figure 4). During
539 exposure to FNA, *D. vulgaris* switched from a status of prolific growth to a phase of
540 severely inhibited growth. When exposed to FNA at 4.0 μg N/L sulfate reduction and
541 lactate oxidation coupled with ATP generation were suppressed, leading to energy
542 starvation in the FNA-added cultures. Expression of genes coding for lactate
543 oxidation and sulfate reduction were subsequently lowered. In response to energy
544 starvation, *D. vulgaris* stabilised its existing ribosomes and ceased translation of
545 proteins. In addition, FNA caused more oxidative conditions in *D. vulgaris* and there
546 was transcriptional evidence of attempts to alleviate the oxidative stress. The findings
547 of this study not only provide insight and fundamental understanding of the

548 antimicrobial mechanism of FNA, but also can assist in the application of FNA in real
549 sewers for control of sulfide production and corrosion,
550

551 ## Acknowledgment

552 We acknowledge the Australian Research Council for funding support through project
553 DP120102832 (Biofilm Control in Wastewater Systems using Free Nitrous Acid - a
554 Renewable Material from Wastewater) and we thank the China Scholarship Council
555 for scholarship support for Shu-Hong Gao. We thank Dr. Beatrice Keller, Jianguang
556 Li, University of Queensland for IC and HPLC analysis and Dr. Michael Nefedov,
557 University of Queensland for assistance with the BD FACSAria™ II flow cytometer
558 and data analysis.
559

560 ## References

561 1. **Jiang G, Keating A, Corrie S, O'halloran K, Nguyen L, Yuan Z.** 2013.
562 Dosing free nitrous acid for sulfide control in sewers: Results of field trials in
563 Australia. Water Res **47:**4331-4339.
564 2. **Heidelberg JF, Seshadri R, Haveman SA, Hemme CL, Paulsen IT,**
565 **Kolonay JF, Eisen JA, Ward N, Methe B, Brinkac LM, Daugherty SC,**
566 **Deboy RT, Dodson RJ, Durkin AS, Madupu R, Nelson WC, Sullivan SA,**
567 **Fouts D, Haft DH, Selengut J, Peterson JD, Davidsen TM, Zafar N, Zhou**
568 **L, Radune D, Dimitrov G, Hance M, Tran K, Khouri H, Gill J, Utterback**
569 **TR, Feldblyum TV, Wall JD, Voordouw G, Fraser CM.** 2004. The genome
570 sequence of the anaerobic, sulfate-reducing bacterium *Desulfovibrio vulgaris*
571 Hildenborough. Nat Biotechnol **22:**554-559.

572 3. **Jiang G, Gutierrez O, Yuan Z.** 2011. The strong biocidal effect of free
573 nitrous acid on anaerobic sewer biofilms. Water Res **45:**3735-3743.
574 4. **Pikaar I, Sharma KR, Hu S, Gernjak W, Keller J, Yuan Z.** 2014. Water
575 engineering. Reducing sewer corrosion through integrated urban water
576 management. Science **345:**812-814.
577 5. **Gutierrez O, Mohanakrishnan J, Sharma KR, Meyer RL, Keller J, Yuan**
578 **Z.** 2008. Evaluation of oxygen injection as a means of controlling sulfide
579 production in a sewer system. Water Res **42:**4549-4561.
580 6. **Mohanakrishnan J, Gutierrez O, Sharma KR, Guisasola A, Werner U,**
581 **Meyer RL, Keller J, Yuan Z.** 2009. Impact of nitrate addition on biofilm
582 properties and activities in rising main sewers. Water Res **43:**4225-4237.
583 7. **Zhang L, Keller J, Yuan Z.** 2009. Inhibition of sulfate-reducing and
584 methanogenic activities of anaerobic sewer biofilms by ferric iron dosing.
585 Water Res **43:**4123-4132.
586 8. **Gutierrez O, Park D, Sharma KR, Yuan Z.** 2009. Effects of long-term pH
587 elevation on the sulfate-reducing and methanogenic activities of anaerobic
588 sewer biofilms. Water Res **43:**2549-2557.
589 9. **Zhang L, B DG, P DS, Mendoza L, Marzorati M, Verstraete W.** 2009.
590 Decreasing sulfide generation in sewage by dosing formaldehyde and its
591 derivatives under anaerobic conditions. Water Sci Technol **59:**1248-1254.
592 10. **Jiang G, Gutierrez O, Sharma KR, Keller J, Yuan Z.** 2011. Optimization
593 of intermittent, simultaneous dosage of nitrite and hydrochloric acid to control
594 sulfide and methane productions in sewers. Water Res **45:**6163-6172.

595 11. **Vadivelu VM, Yuan Z, Fux C, Keller J.** 2006. The inhibitory effects of free
596 nitrous acid on the energy generation and growth processes of an enriched
597 nitrobacter culture. Environ Sci Technol **40:**4442-4448.
598 12. **Haveman SA, Greene EA, Stilwell CP, Voordouw JK, Voordouw G.** 2004.
599 Physiological and gene expression analysis of inhibition of *Desulfovibrio*
600 *vulgaris* Hildenborough by nitrite. J Bacteriol **186:**7944-7950.
601 13. **He Q, Huang KH, He Z, Alm EJ, Fields MW, Hazen TC, Arkin AP, Wall**
602 **JD, Zhou J.** 2006. Energetic consequences of nitrite stress in *Desulfovibrio*
603 *vulgaris* Hildenborough, inferred from global transcriptional analysis. Appl
604 Environ Microbiol **72:**4370-81.
605 14. **Fang FC.** 2004. Antimicrobial reactive oxygen and nitrogen species: concepts
606 and controversies. Nat Rev Microbiol **2:**820-832.
607 15. **Zahrt TC, Deretic V.** 2002. Reactive nitrogen and oxygen intermediates and
608 bacterial defenses: unusual adaptations in *Mycobacterium tuberculosis*.
609 Antioxid Redox Signal **4:**141-159.
610 16. **Zhou Y, Oehmen A, Lim M, Vadivelu V, Ng WJ.** 2011. The role of nitrite
611 and free nitrous acid (FNA) in wastewater treatment plants. Water Res
612 **45:**4672-4682.
613 17. **O'Leary V, Solberg M.** 1976. Effect of sodium nitrite inhibition on
614 intracellular thiol groups and on the activity of certain glycolytic enzymes in
615 *Clostridium perfringens*. Appl Environ Microbiol **31:**208-212.
616 18. **Wang Q, Ye L, Jiang G, Hu S, Yuan Z.** 2014. Side-stream sludge treatment
617 using free nitrous acid selectively eliminates nitrite oxidizing bacteria and
618 achieves the nitrite pathway. Water Res **55:**245-255.

19. **Sun J, Hu S, Sharma KR, Ni BJ, Yuan Z.** 2014. Stratified microbial structure and activity in sulfide- and methane-producing anaerobic sewer biofilms. Appl Environ Microbiol **80:**7042-7052.
20. **Pereira IA, LeGall J, Xavier AV, Teixeira M.** 2000. Characterization of a heme c nitrite reductase from a non-ammonifying microorganism, *Desulfovibrio vulgaris* Hildenborough. Biochim Biophys Acta **1481:**119-130.
21. **Korte HL, Saini A, Trotter VV, Butland GP, Arkin AP, Wall JD.** 2015. Independence of nitrate and nitrite inhibition of *Desulfovibrio vulgaris* Hildenborough and use of nitrite as a substrate for growth. Environ Sci Technol **49:**924-931.
22. **Zhou AF, He ZL, Redding-Johanson AM, Mukhopadhyay A, Hemme CL, Joachimiak MP, Luo F, Deng Y, Bender KS, He Q, Keasling JD, Stahl DA, Fields MW, Hazen TC, Arkin AP, Wall JD, Zhou JZ.** 2010. Hydrogen peroxide-induced oxidative stress responses in *Desulfovibrio vulgaris* Hildenborough. Environ Microbiol **12:**2645-2657.
23. **Gao S-H, Fan L, Yuan Z, Bond PL.** 2015. The concentration-determined and population-specific antimicrobial effects of free nitrous acid on *Pseudomonas aeruginosa* PAO1. Appl Microbiol Biotechnol **99:**2305-2312.
24. **Keller-Lehmann B., Corrie S., Ravn R., Yuan Z., and Keller J.** 2006. Preservation and simultaneous analysis of relevant soluble sulfur species in sewage samples. Proceedings of the Second International IWA Conference on Sewer Operation and Maintenance, Vienna, Austria.
25. **Gao S-H, Fan L, Peng L, Guo J, Agulló-Barceló M, Yuan Z, Bond PL.** 2016. Determining multiple responses of *Pseudomonas aeruginosa* PAO1 to an antimicrobial agent, free nitrous acid. Environ Sci Technol **50:**5305-5312.

644 26. **Patel RK, Jain M.** 2012. NGS QC Toolkit: a toolkit for quality control of
645 next generation sequencing data. PLoS One **7:**e30619.
646 27. **Mu JC, Jiang H, Kiani A, Mohiyuddin M, Bani Asadi N, Wong WH.** 2012.
647 Fast and accurate read alignment for resequencing. Bioinformatics **28:**2366-
648 2373.
649 28. **Trapnell C, Roberts A, Goff L, Pertea G, Kim D, Kelley DR, Pimentel H,**
650 **Salzberg SL, Rinn JL, Pachter L.** 2012. Differential gene and transcript
651 expression analysis of RNA-seq experiments with TopHat and Cufflinks. Nat
652 Protoc **7:**562-578.
653 29. **Poole RK.** 2005. Nitric oxide and nitrosative stress tolerance in bacteria.
654 Biochem Soc Trans **33:**176-180.
655 30. **Bykov D, Neese F.** 2015. Six-Electron reduction of nitrite to ammonia by
656 cytochrome c nitrite reductase: insights from density functional theory studies.
657 Inorg Chem **54:**9303-9316.
658 31. **Wolfe MT, Heo J, Garavelli JS, Ludden PW.** 2002. Hydroxylamine
659 reductase activity of the hybrid cluster protein from *Escherichia coli*. J
660 Bacteriol **184:**5898-5902.
661 32. **Vita N, Valette O, Brasseur G, Lignon S, Denis Y, Ansaldi M, Dolla A,**
662 **Pieulle L.** 2015. The primary pathway for lactate oxidation in *Desulfovibrio*
663 *vulgaris*. Front Microbiol **6:**606.
664 33. **Agafonov DE, Kolb VA, Spirin AS.** 2001. A novel stress-response protein
665 that binds at the ribosomal subunit interface and arrests translation. Cold
666 Spring Harb Symp Quant Biol **66:**509-514.

34. **Srinivasan SR, Gillies AT, Chang L, Thompson AD, Gestwicki JE.** 2012. Molecular chaperones DnaK and DnaJ share predicted binding sites on most proteins in the *E. coli* proteome. Mol Biosyst **8:**2323-2333.

35. **Aragao D, Mitchell EP, Frazao CF, Carrondo MA, Lindley PF.** 2008. Structural and functional relationships in the hybrid cluster protein family: structure of the anaerobically purified hybrid cluster protein from *Desulfovibrio vulgaris* at 1.35 angstrom resolution. Acta Cryst D **64:**665-674.

36. **Kim JH, Akagi JM.** 1985. Characterization of a trithionate reductase system from *Desulfovibrio vulgaris*. J Bacteriol **163:**472-475.

37. **Rabus R., Hansen T. A., and Widdel F.** 2006. Dissimilatory sulfate-and sulfur-reducing prokaryotes, p 659-660. *In* R. Rabus, T. A. Hansen and F. Widdel (ed.). The prokaryotes. Springer-Verlag, New York, N.Y.

38. **Tibelius KH, Knowles R.** 1984. Hydrogenase activity in *Azospirillum brasilense* is inhibited by nitrite, nitric oxide, carbon monoxide, and acetylene. J Bacteriol **160:**103-106.

39. **Mühlig A, Behr J, Scherer S, Müller-Herbst S.** 2014. Stress response of *Salmonella enterica serovar* typhimurium to acidified nitrite. Appl Environ Microbiol **80:**6373-6382.

40. **Jiang G, Yuan Z.** 2013. Synergistic inactivation of anaerobic wastewater biofilm by free nitrous acid and hydrogen peroxide. J Hazard Mater **250-251:**91-98.

41. **Moran MA, Satinsky B, Gifford SM, Luo H, Rivers A, Chan LK, Meng J, Durham BP, Shen C, Varaljay VA, Smith CB, Yager PL, Hopkinson BM.** 2013. Sizing up metatranscriptomics. ISME J **7:**237-243.

**Figure 1.** Growth profiles of *D. vulgaris* batch cultures in the presence of different starting FNA concentrations (μg N/L). FNA was added at time 0 h. The control culture has no FNA addition. Error bars show the standard deviation of the triplicated cultures. The figure legend shows the FNA starting concentrations.

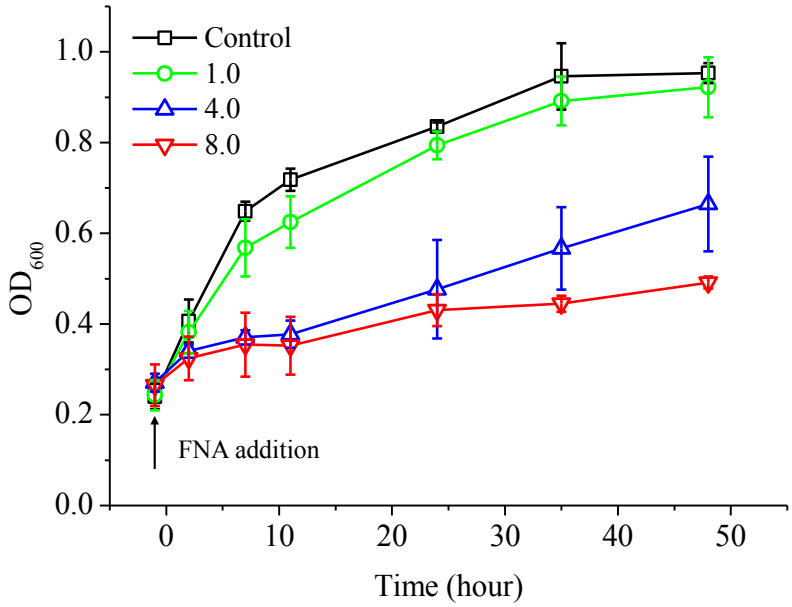

Figure 2. Levels of nitrite (A), FNA (B), lactate (C), acetate (D), sulfate (E), sulfide (F), sulfite (G), and thiosulfate (H) in *D. vulgaris* batch cultures grown on lactate and sulfate. The batch cultures were exposed to different levels of FNA that was added at time 0 h, which was 26 hours after inoculation. No FNA was added to the control cultures. Error bars represent the standard deviation of analyses performed from triplicate batch cultures. The figure legend shows the FNA starting concentrations (µg N/L).

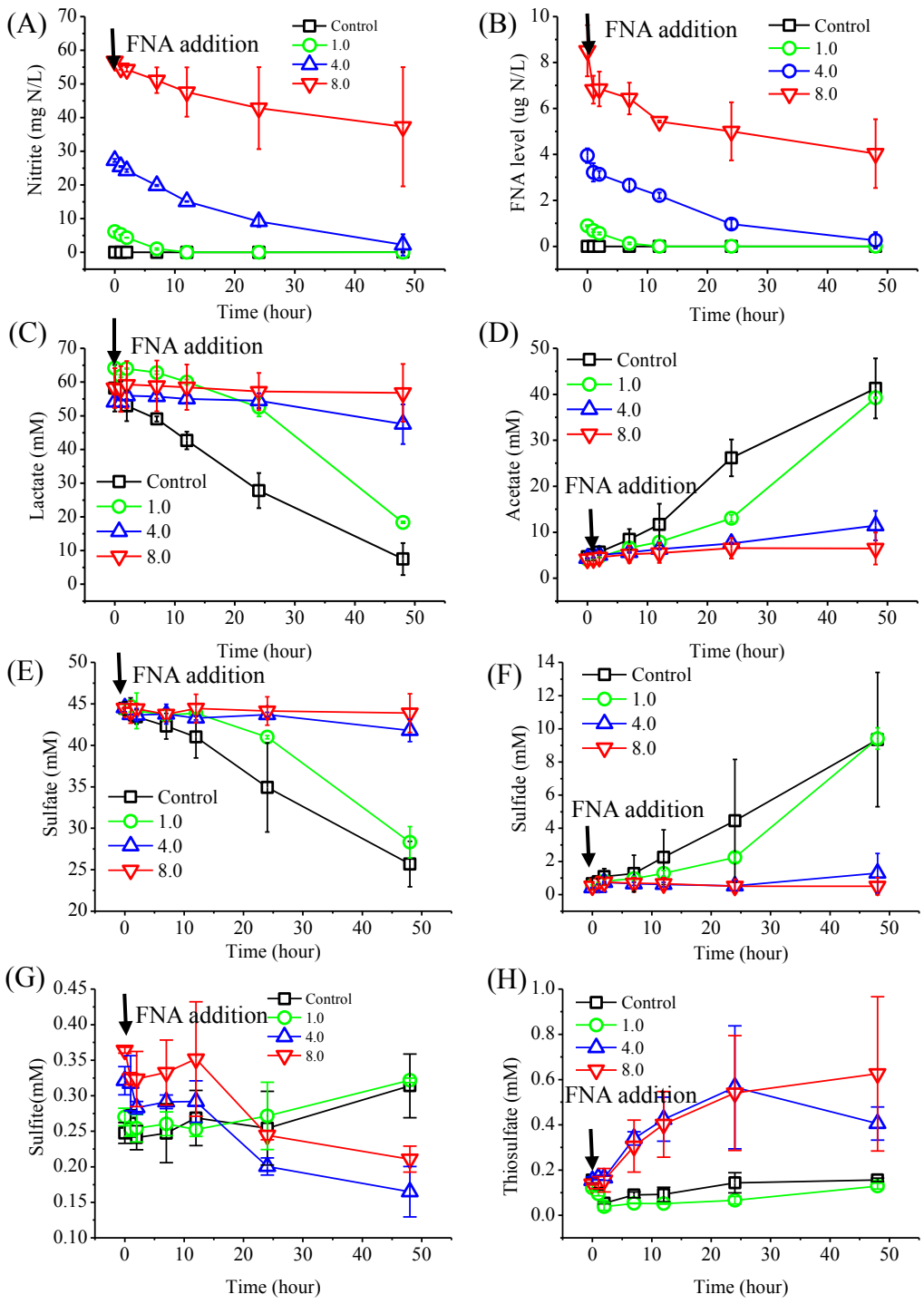
(A)
Nitrite (mg N/L)
FNA addition
Control
1.0
4.0
8.0
Time (hour)
(B)
FNA level (ug N/L)
FNA addition
Control
1.0
4.0
8.0
Time (hour)
(C)
Lactate (mM)
FNA addition
Control
1.0
4.0
8.0
Time (hour)
(D)
Acetate (mM)
Control
1.0
4.0
8.0
FNA addition
Time (hour)
(E)
Sulfate (mM)
FNA addition
Control
1.0
4.0
8.0
Time (hour)
(F)
Sulfide (mM)
Control
1.0
4.0
8.0
FNA addition
Time (hour)
(G)
Sulfite(mM)
FNA addition
Control
1.0
4.0
8.0
Time (hour)
(H)
Thiosulfate (mM)
Control
1.0
4.0
8.0
FNA addition
Time (hour)

704

Figure 3. Physiological features of *D. vulgaris* measured during the batch cultures incubations in the presence of different starting FNA levels and when no FNA was added (control). The percentage of live cells (A), cellular thiol levels (B), intracellular redox levels, where higher fluorescence indicates lower redox potential (C), and cellular ATP levels (D). FNA was added at time 0 h. Error bars represent the standard deviation of analyses performed from triplicate batch cultures. The figure legend shows the FNA starting concentrations (μg N/L).

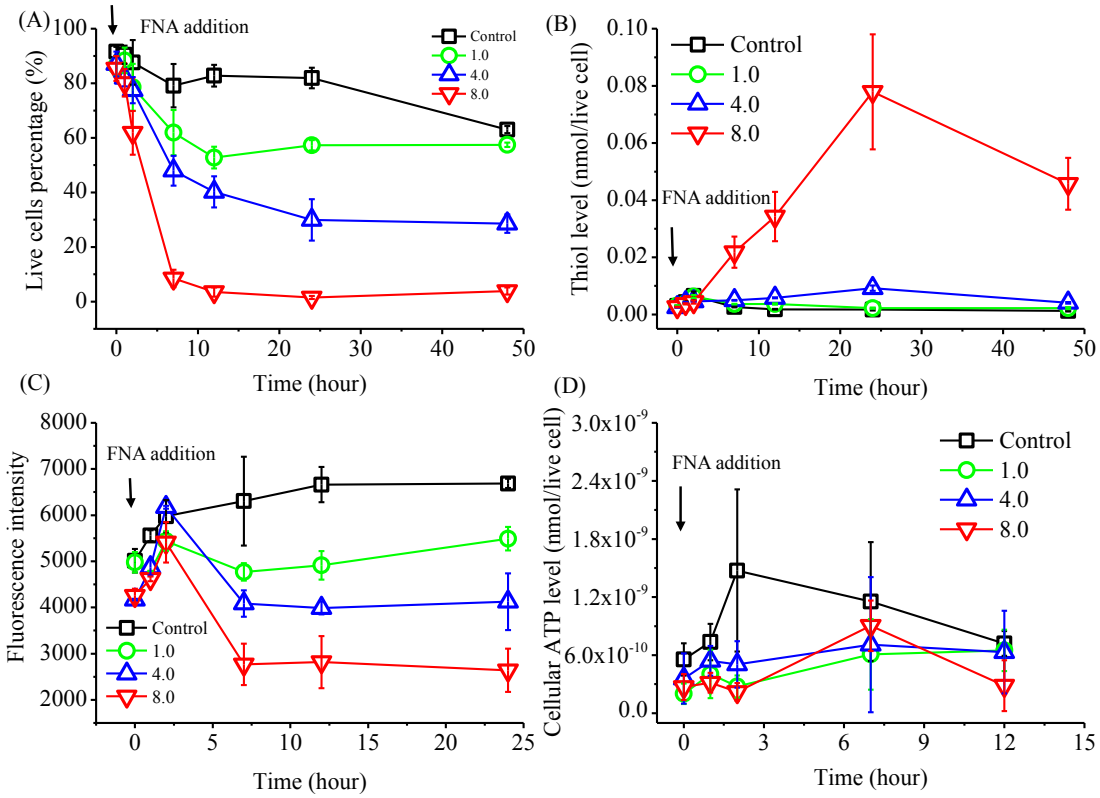

Figure 4. Proposed antimicrobial effects of FNA on *D. vulgaris* based on interpretations of measured physiological activities and the transcriptional responses. The colored boxes indicate activities or events where the associated gene expression was primarily increased (blue) or decreased (pink) in response to FNA exposure.

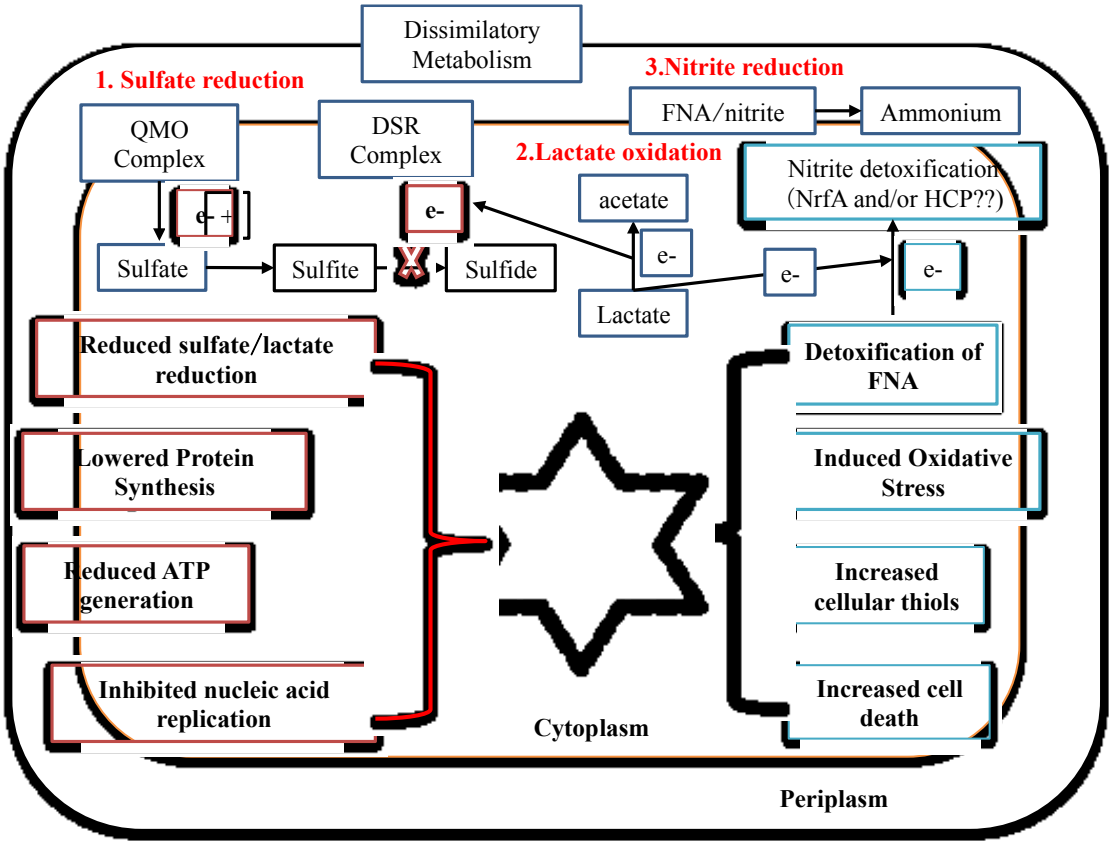

718 Table 1. Absolute ratios of lactate and sulfate used and acetate produced during the 48

719 h incubation of *D. vulgarius* cultures in the presence and absence of added FNA.

| Culture condition | Lactate used (mM) | Sulfate used (mM) | Acetate produced (mM) |
|---|---|---|---|
| [a] Theoretical ratio | 2 | 1 | 2 |
| Control, no FNA | 3.00±1.17 | 1.00±0.31 | 2.60±1.21 |
| FNA at 1.0 μg N/L | 2.83±0.13 | 1.00±0.08 | 2.19±0.00 |
| FNA at 4.0 μg N/L | 3.00±0.31 | 1.00±0.27 | 2.61±0.59 |
| FNA at 8.0 μg N/L | 3.51±1.56 | 1.00±1.17 | 3.44±1.49 |

720 [a] The theoretical ratio based on the stoichiometry if acetate is the product.

721 Table 2. The transcriptional responses of *D. vulgaris* genes involved in detoxification when exposed to FNA for 1 h with an initial concentration

722 of 4.0 μg N/L.

| Gene ID | Gene name | Annotation | RPKM_Control | RPKM_FNA-added | LFC | Fold change | q value |
|---|---|---|---|---|---|---|---|
| Oxidative stress | | | | | | | |
| DVU2247 | ahpC | anti-oxidant AhpCTSA family protein | 643.79 | 2376.65 | 1.88 | 3.68 | 0.0003 |
| DVU1397 | bfr | bacterioferritin | 148.13 | 381.75 | 1.37 | 2.58 | 0.0003 |
| DVU3183 | sor | desulfoferrodoxin | 1237.40 | 3966.13 | 1.68 | 3.21 | 0.0003 |
| DVU0772 | | Hypothetical Protein | 1622.19 | 8374.84 | 2.37 | 5.17 | 0.0003 |
| DVU0576 | msrB | methionine sulfoxide reductase B | 15.78 | 649.09 | 5.36 | 41.07 | 0.0003 |
| DVU1984 | msrA | peptide methionine sulfoxide reductase MsrA | 24.08 | 181.96 | 2.92 | 7.57 | 0.0003 |
| DVU1457 | trxB | thioredoxin reductase | 81.88 | 415.55 | 2.34 | 5.08 | 0.0003 |
| Fur Regulon | | | | | | | |
| DVU0942 | fur | Fur family transcriptional regulator | 199.36 | 340.38 | 0.77 | 1.71 | 0.0241 |
| DVU2574 | | Ferrous Ion Transport Protein | 123.57 | 708.01 | 2.52 | 5.74 | 0.0003 |
| DVU2680 | fld | Flavodoxin, iron-repressed | 166.69 | 1892.42 | 3.50 | 11.31 | 0.0003 |
| DVU0763 | gdp | Diguanylate Cyclase | 21.37 | 185.5 | 3.12 | 8.69 | 0.0003 |
| DVU0273 | | Conserved hypothetical Protein | 37.96 | 244.7 | 2.69 | 6.45 | 0.0003 |
| Nitrite reduction | | | | | | | |
| DVU0625 | | Cytochrome c Nitrite Reductase, Catalytic Subunit NfrA | 94.88 | 1874.77 | 4.30 | 19.70 | 0.6357 |
| DVU2543 | | Hydroxylamine Reductase | 8.44 | 8588.86 | 9.99 | 1016.93 | 0.0003 |
| DVU2544 | | iron-sulfur cluster-binding protein | 4.29 | 1133.96 | 8.05 | 264.58 | 0.0003 |

723

724 Table 3. FNA effects on the transcriptional responses of *D. vulgaris* genes involved in metabolism when exposed to FNA for 1 h with an initial

725 concentration of 4.0 µg N/L [a].

| Gene ID | Gene name | Annotation | RPKM_Control | RPKM_FNA-added | LFC | Fold change | q value |
|---|---|---|---|---|---|---|---|
| Sulfate reduction | | | | | | | |
| DVU0847 | apsA | adenylylsulfate reductase subunit alpha | 6909.68 | 5078.47 | -0.44 | -1.36 | 0.3464 |
| DVU0846 | apsB | adenylylsulfate reductase subunit beta | 9741.20 | 7860.48 | -0.31 | -1.24 | 0.5378 |
| DVU1288 | dsrJ | Cytochrome c family protein (DsrJ) | 534.27 | 61.42 | -3.12 | -8.70 | 0.6528 |
| DVU0402 | dsrA | dissimilatory sulfite reductase subunit alpha | 2089.97 | 985.96 | -1.08 | -2.12 | 0.0128 |
| DVU0403 | dsrB | dissimilatory sulfite reductase subunit beta | 2141.02 | 1348.20 | -0.67 | -1.59 | 0.1274 |
| DVU0848 | | Heterodisulfide Reductase (Qmo) | 926.97 | 528.78 | -0.81 | -1.75 | 0.0488 |
| DVU0849 | | Heterodisulfide Reductase, Iron-Sulfur-Binding Subunit (Qmo) | 559.5 | 223.45 | -1.32 | -2.50 | 0.0035 |
| DVU0850 | | Heterodisulfide Reductase, Transmembrane Subunit (Qmo) | 705.61 | 301.39 | -1.23 | -2.35 | 0.0042 |
| DVU1290 | dsrM | nitrate reductase subunit gamma (DsrM) | 812.85 | 115.61 | -2.81 | -7.03 | 0.0003 |
| DVU1289 | dsrK | reductase, iron-sulfur binding subunit (DsrK) | 344.44 | 48.62 | -2.82 | -7.08 | 0.0003 |
| DVU1287 | dsrO | reductase, iron-sulfur binding subunit (DsrO) | 366.72 | 53.15 | -2.79 | -6.90 | 0.6170 |
| DVU1286 | dsrP | reductase, transmembrane subunit (DsrP) | 423.76 | 69.34 | -2.61 | -6.11 | 0.0003 |
| DVU1597 | sir | sulfite reductase, assimilatory-type | 216.21 | 113.30 | -0.93 | -1.91 | 0.0051 |
| Lactate oxidation | | | | | | | |
| DVU3030 | ackA | acetate kinase | 339.10 | 83.54 | -2.02 | -4.06 | 0.0003 |
| DVU3027 | glcD | glycolate oxidase subunit GlcD | 274.79 | 125.67 | -1.13 | -2.19 | 0.0035 |
| DVU3031 | | hypothetical protein DVU3031 | 136.07 | 17.79 | -2.93 | -7.65 | 0.6411 |
| DVU3032 | | hypothetical protein DVU3032 | 511.29 | 42.46 | -3.59 | -12.04 | 0.6108 |
| DVU3028 | | iron-sulfur cluster-binding protein | 281.53 | 136.67 | -1.04 | -2.06 | 0.0037 |

| | | | | | | | |
|---|---|---|---|---|---|---|---|
| DVU3033 | | iron-sulfur cluster-binding protein | 273.18 | 30.99 | -3.14 | -8.82 | 0.0003 |
| DVU0600 | | L-lactate Dehydrogenase | 5.29 | 25.03 | 2.24 | 4.72 | 0.0003 |
| DVU2110 | | L-lactate permease | 5.39 | 5.63 | 0.06 | 1.04 | 0.9109 |
| DVU2285 | | L-lactate permease | 111.29 | 27.81 | -2.00 | -4.00 | 0.0003 |
| DVU2451 | | L-lactate permease | 281.30 | 156.81 | -0.84 | -1.79 | 0.0229 |
| DVU2683 | | L-lactate permease | 118.96 | 20.57 | -2.53 | -5.78 | 0.0003 |
| DVU3026 | | L-lactate permease | 121.11 | 77.86 | -0.64 | -1.56 | 0.0639 |
| DVU3029 | pta | phosphate acetyltransferase | 236.08 | 75.62 | -1.64 | -3.12 | 0.0003 |
| DVU1569 | porA | pyruvate ferredoxin oxidoreductase subunit alpha | 40.03 | 20.68 | -0.95 | -1.94 | 0.7719 |
| DVU1570 | porB | pyruvate ferredoxin oxidoreductase subunit beta | 42.03 | 26.86 | -0.65 | -1.56 | 0.8398 |
| DVU3025 | poR | pyruvate-ferredoxin oxidoreductase | 821.96 | 337.59 | -1.28 | -2.43 | 0.7256 |
| DVU0577 | | formate dehydrogenase formation protein FdhE | 22.78 | 53.38 | 1.23 | 2.35 | 0.0012 |
| DVU0587 | fdnG-1 | formate dehydrogenase subunit alpha | 48.25 | 203.16 | 2.07 | 4.20 | 0.0003 |
| DVU0588 | | formate dehydrogenase subunit beta | 77.04 | 318.11 | 2.05 | 4.14 | 0.0003 |
| | | | | | | | |
| ATP synthesis | | | | | | | |
| DVU0918 | atpB | ATP synthase F0 subunit A | 938.08 | 160.96 | -2.54 | -5.83 | 0.0003 |
| DVU0779 | atpF | ATP synthase F0 subunit B | 1224.30 | 266.04 | -2.20 | -4.60 | 0.6435 |
| DVU0780 | | ATP synthase F0 subunit B\' | 730.80 | 226.18 | -1.69 | -3.23 | 0.0003 |
| DVU0920 | atpI | ATP synthase I | 956.69 | 313.18 | -1.61 | -3.05 | 0.6970 |
| DVU0777 | atpA | F0F1 ATP synthase subunit alpha | 1156.37 | 198.62 | -2.54 | -5.82 | 0.0003 |
| DVU0775 | atpD | F0F1 ATP synthase subunit beta | 1069.12 | 186.45 | -2.52 | -5.73 | 0.0003 |
| DVU0778 | atpH | F0F1 ATP synthase subunit delta | 1589.63 | 295.74 | -2.43 | -5.38 | 0.6396 |
| DVU0774 | atpC | F0F1 ATP synthase subunit epsilon | 1510.29 | 345.95 | -2.13 | -4.37 | 0.0003 |
| DVU0776 | atpG | F0F1 ATP synthase subunit gamma | 1369.15 | 214.02 | -2.68 | -6.40 | 0.0003 |
| | | | | | | | |
| Electron transfer | | | | | | | |

| | | | | | | | |
|---|---|---|---|---|---|---|---|
| DVU2524 | | cytochrome c3, putative | 2.70 | 3.15 | 0.22 | 1.17 | 1 |
| DVU0434 | | ech hydrogenase subunit EchA | 12.66 | 3.28 | -1.95 | -3.86 | 0.6701 |
| DVU0433 | | ech hydrogenase subunit EchB | 11.18 | 2.20 | -2.34 | -5.07 | 0.5587 |
| DVU0432 | | ech hydrogenase subunit EchC | 15.72 | 5.16 | -1.61 | -3.05 | 0.0431 |
| DVU0431 | | ech hydrogenase subunit EchD | 22.67 | 6.16 | -1.88 | -3.68 | 0.0163 |
| DVU0430 | | ech hydrogenase subunit EchE | 13.88 | 5.16 | -1.43 | -2.69 | 0.0066 |
| DVU0429 | | ech hydrogenase subunit EchF | 13.21 | 5.81 | -1.19 | -2.28 | 0.1921 |
| DVU2796 | | electron transport complex protein RnfA | 46.78 | 33.47 | -0.48 | -1.40 | 0.2438 |
| DVU2792 | | electron transport complex protein RnfC | 45.12 | 43.07 | -0.07 | -1.05 | 0.8732 |
| DVU2793 | | electron transport complex protein RnfD | 20.48 | 18.30 | -0.16 | -1.12 | 0.7781 |
| DVU2794 | | electron transport complex protein RnfG | 32.95 | 30.79 | -0.10 | -1.07 | 0.8453 |
| DVU0535 | | Hmc Operon Protein 2 | 15.05 | 38.37 | 1.35 | 2.55 | 0.0003 |
| DVU0534 | | Hmc Operon Protein 3 | 12.24 | 37.62 | 1.62 | 3.07 | 0.0003 |
| DVU0532 | | Hmc Operon Protein 5 | 10.58 | 32.98 | 1.64 | 3.12 | 0.0003 |
| DVU0531 | | Hmc Operon Protein 6 | 14.61 | 45.6 | 1.64 | 3.12 | 0.0003 |
| | | | | | | | |
| Hydrogenases | | | | | | | |
| DVU1769 | hydA | Periplasmic [FeFe] Hydrogenase, Large Subunit | 17.53 | 8.14 | -1.11 | -2.16 | 0.009 |
| DVU1770 | hydB | periplasmic [FeFe] hydrogenase, small subunit | 12.08 | 8.55 | -0.50 | -1.41 | 0.6281 |
| DVU2526 | hynA-2 | periplasmic [NiFe] hydrogenase, large unit, isozyme 2 | 3.36 | 4.67 | 0.47 | 1.39 | 0.3684 |
| DVU2525 | hynB-2 | periplasmic [NiFe] hydrogenase, small unit, isozyme 2 | 2.26 | 3.00 | 0.41 | 1.33 | 1 |
| DVU1918 | hysA | Periplasmic [NiFeSe] hydrogenase, Large Subunit | 575.74 | 265.41 | -1.12 | -2.17 | 0.0062 |
| DVU1917 | hysB | Periplasmic [NiFeSe] Hydrogenase, Small Subunit | 706.06 | 236.22 | -1.58 | -2.99 | 0.0003 |

[a] Note: Some genes included in the table were not differentially expressed according to the applied criteria of LFC (see materials and methods section) but were included here to aid illustration of an FNA affected pathway or mechanism.

728 Table 4. FNA effects on the transcriptional responses of *D. vulgaris* genes involved in DNA replication, transcription and translation when

729 exposed to FNA for 1 h with an initial concentration of 4.0 μg N/L.

| Gene ID | Gene name | Annotation | RPKM_Control | RPKM_FNA-added | LFC | Fold change | q value |
|---|---|---|---|---|---|---|---|
| DVU1469 | rpsA | 30S ribosomal protein S1 | 66.08 | 31.43 | -1.07 | -2.10 | 0.0012 |
| DVU1302 | rpsJ | 30S ribosomal protein S10 | 2247.95 | 749.15 | -1.59 | -3.00 | 0.0003 |
| DVU1327 | rpsK | 30S ribosomal protein S11 | 1785.05 | 802.95 | -1.15 | -2.22 | 0.0022 |
| DVU1298 | rpsL | 30S ribosomal protein S12 | 1605.02 | 539.75 | -1.57 | -2.97 | 0.0003 |
| DVU1326 | rpsM | 30S ribosomal protein S13 | 1579.22 | 661.60 | -1.26 | -2.39 | 0.0008 |
| DVU1316 | rpsN | 30S ribosomal protein S14 | 2500.39 | 558.05 | -2.16 | -4.48 | 0.0003 |
| DVU0839 | rpsP | 30S ribosomal protein S16 | 1897.36 | 902.76 | -1.07 | -2.10 | 0.0024 |
| DVU0874 | rpsB | 30S ribosomal protein S2 | 568.75 | 187.39 | -1.60 | -3.04 | 0.0003 |
| DVU1896 | rpsT | 30S ribosomal protein S20 | 1074.90 | 347.59 | -1.63 | -3.09 | 0.0003 |
| DVU1309 | rpsC | 30S ribosomal protein S3 | 1612.99 | 373.63 | -2.11 | -4.32 | 0.0003 |
| DVU1328 | rpsD | 30S ribosomal protein S4 | 1832.03 | 702.74 | -1.38 | -2.61 | 0.0010 |
| DVU1320 | rpsE | 30S ribosomal protein S5 | 1254.60 | 345.84 | -1.86 | -3.63 | 0.0003 |
| DVU0956 | rpsF | 30S ribosomal protein S6 | 846.18 | 368.63 | -1.20 | -2.30 | 0.0003 |
| DVU1299 | rpsG | 30S ribosomal protein S7 | 1661.83 | 516.48 | -1.69 | -3.22 | 0.0003 |
| DVU1317 | rpsH | 30S ribosomal protein S8 | 1628.86 | 350.60 | -2.22 | -4.65 | 0.0003 |
| DVU2925 | rplA | 50S ribosomal protein L1 | 1207.01 | 322.34 | -1.90 | -3.74 | 0.0003 |
| DVU2926 | rplJ | 50S ribosomal protein L10 | 2811.97 | 704.14 | -2.00 | -3.99 | 0.0003 |
| DVU2924 | rplK | 50S ribosomal protein L11 | 2152.09 | 479.63 | -2.17 | -4.49 | 0.0003 |
| DVU2518 | rplM | 50S ribosomal protein L13 | 2740.46 | 1358.38 | -1.01 | -2.02 | 0.0135 |
| DVU1313 | rplN | 50S ribosomal protein L14 | 2360.35 | 587.04 | -2.01 | -4.02 | 0.0003 |
| DVU1310 | rplP | 50S ribosomal protein L16 | 2220.49 | 487.73 | -2.19 | -4.55 | 0.0003 |
| DVU1319 | rplR | 50S ribosomal protein L18 | 1455.69 | 380.51 | -1.94 | -3.83 | 0.0003 |

| | | | | | | | |
|---|---|---|---|---|---|---|---|
| DVU0835 | rplS | 50S ribosomal protein L19 | 2049.36 | 953.53 | -1.10 | -2.15 | 0.0037 |
| DVU1306 | rplB | 50S ribosomal protein L2 | 1281.60 | 385.53 | -1.73 | -3.32 | 0.0003 |
| DVU2535 | rplT | 50S ribosomal protein L20 | 1552.62 | 508.75 | -1.61 | -3.05 | 0.0003 |
| DVU0927 | rplU | 50S ribosomal protein L21 | 1418.19 | 648.20 | -1.13 | -2.19 | 0.0020 |
| DVU1308 | rplV | 50S ribosomal protein L22 | 2353.89 | 499.49 | -2.24 | -4.71 | 0.0003 |
| DVU1574 | rplY | 50S ribosomal protein L25 | 2580.36 | 657.59 | -1.97 | -3.92 | 0.0003 |
| DVU0928 | rpmA | 50S ribosomal protein L27 | 2170.58 | 787.25 | -1.46 | -2.76 | 0.0003 |
| DVU1303 | rplC | 50S ribosomal protein L3 | 2546.31 | 731.53 | -1.80 | -3.48 | 0.0003 |
| DVU1315 | rplE | 50S ribosomal protein L5 | 3189.91 | 604.46 | -2.40 | -5.28 | 0.0003 |
| DVU1318 | rplF | 50S ribosomal protein L6 | 2154.53 | 518.55 | -2.05 | -4.15 | 0.0003 |
| DVU2927 | rplL | 50S ribosomal protein L7/L12 | 4245.40 | 1100.25 | -1.95 | -3.86 | 0.0003 |
| DVU1089 | alaS | alanyl-tRNA synthetase | 69.54 | 16.30 | -2.09 | -4.27 | 0.0003 |
| DVU3166 | | alanyl-tRNA synthetase | 18.77 | 2.35 | -2.99 | -7.97 | 0.0096 |
| DVU1248 | argS | arginyl-tRNA synthetase | 108.21 | 39.12 | -1.47 | -2.77 | 0.0003 |
| DVU3367 | aspS | aspartyl-tRNA synthetase | 87.97 | 24.05 | -1.87 | -3.66 | 0.0003 |
| DVU0808 | gatA | aspartyl/glutamyl-tRNA amidotransferase subunit A | 31.75 | 6.67 | -2.25 | -4.76 | 0.0003 |
| DVU1885 | gatB | aspartyl/glutamyl-tRNA amidotransferase subunit B | 72.54 | 27.09 | -1.42 | -2.68 | 0.0003 |
| DVU0001 | dnaA-1 | chromosomal replication initiator protein DnaA | 42.34 | 14.96 | -1.50 | -2.83 | 0.0003 |
| DVU2252 | dnaA-2 | chromosomal replication initiator protein DnaA | 108.04 | 45.84 | -1.24 | -2.36 | 0.0005 |
| DVU0004 | gyrA | DNA gyrase subunit A | 71.66 | 10.01 | -2.84 | -7.16 | 0.0003 |
| DVU0003 | gyrB | DNA gyrase subunit B | 76.62 | 12.47 | -2.62 | -6.14 | 0.0003 |
| DVU0483 | mutL | DNA mismatch repair protein MutL | 10.08 | 34.23 | 1.76 | 3.40 | 0.0003 |
| DVU0002 | dnaN | DNA polymerase III subunit beta | 190.12 | 35.75 | -2.41 | -5.32 | 0.0003 |
| DVU1193 | radC | DNA repair protein RadC | 38.21 | 109.95 | 1.52 | 2.88 | 0.0003 |
| DVU1899 | | DNA repair protein RecO | 17.57 | 3.75 | -2.23 | -4.68 | 0.0090 |
| DVU3389 | topA | DNA topoisomerase I | 81.00 | 25.61 | -1.66 | -3.16 | 0.0003 |
| DVU2316 | topB | DNA topoisomerase III | 11.52 | 5.40 | -1.09 | -2.13 | 0.0037 |

| | | | | | | | |
|---|---|---|---|---|---|---|---|
| DVU1730 | | DNA-binding protein | 18.40 | 122.18 | 2.73 | 6.64 | 0.0003 |
| DVU3193 | | DNA-binding protein | 11.67 | 31.95 | 1.45 | 2.74 | 0.0003 |
| DVU0396 | hup-1 | DNA-binding protein HU | 665.69 | 1768.32 | 1.41 | 2.66 | 0.0008 |
| DVU0764 | hup-2 | DNA-binding protein HU | 985.51 | 449.55 | -1.13 | -2.19 | 0.0010 |
| DVU0749 | | DNA-binding response regulator | 4.76 | 17.72 | 1.90 | 3.73 | 0.0003 |
| DVU0596 | lytR | DNA-binding response regulator LytR | 26.69 | 82.99 | 1.64 | 3.11 | 0.0003 |
| DVU2928 | rpoB | DNA-directed RNA polymerase subunit beta | 253.21 | 86.11 | -1.56 | -2.94 | 0.0003 |
| DVU2929 | rpoC | DNA-directed RNA polymerase subunit beta\' | 246.76 | 74.92 | -1.72 | -3.29 | 0.0003 |
| DVU1876 | dnaJ | dnaJ protein | 10.84 | 123.72 | 3.51 | 11.41 | 0.0003 |
| DVU2150 | dnaK | dnaK suppressor protein | 429.45 | 203.48 | -1.08 | -2.11 | 0.0012 |
| DVU3256 | mutM | formamidopyrimidine-DNA glycosylase | 8.23 | 1.51 | -2.45 | -5.45 | 0.0208 |
| DVU2552 | gltX | glutamyl-tRNA synthetase | 52.07 | 24.23 | -1.10 | -2.15 | 0.0018 |
| DVU0809 | gatC | glutamyl-tRNA(Gln) amidotransferase subunit C | 56.08 | 25.83 | -1.12 | -2.17 | 0.0381 |
| DVU1898 | glyQ | glycyl-tRNA synthetase subunit alpha | 124.89 | 42.47 | -1.56 | -2.94 | 0.0003 |
| DVU1897 | glyS | glycyl-tRNA synthetase subunit beta | 56.85 | 16.48 | -1.79 | -3.45 | 0.0003 |
| DVU1927 | ileS | isoleucyl-tRNA synthetase | 108.88 | 40.69 | -1.42 | -2.68 | 0.0003 |
| DVU2376 | lysS | lysyl-tRNA synthetase | 194.54 | 65.27 | -1.58 | -2.98 | 0.0003 |
| DVU0811 | dnaK | molecular chaperone DnaK | 205.16 | 1065.21 | 2.38 | 5.19 | 0.0003 |
| DVU1608 | ligA | NAD-dependent DNA ligase | 21.23 | 4.26 | -2.32 | -4.99 | 0.0003 |
| DVU1573 | pth | peptidyl-tRNA hydrolase | 152.40 | 46.24 | -1.72 | -3.30 | 0.0003 |
| DVU2534 | pheS | phenylalanyl-tRNA synthetase subunit alpha | 145.09 | 29.67 | -2.29 | -4.89 | 0.0003 |
| DVU2533 | pheT | phenylalanyl-tRNA synthetase subunit beta | 68.78 | 13.54 | -2.34 | -5.08 | 0.0003 |
| DVU2904 | | ribosomal RNA large subunit methyltransferase N | 21.51 | 7.33 | -1.55 | -2.93 | 0.0008 |
| DVU1629 | yfiA | ribosomal subunit interface protein | 564.32 | 8136.85 | 3.85 | 14.42 | 0.0003 |
| DVU0897 | | RNA modification protein | 10.62 | 3.19 | -1.74 | -3.33 | 0.0072 |
| DVU1257 | | RNA-binding protein | 1913.15 | 793.62 | -1.27 | -2.41 | 0.0003 |
| DVU2246 | | S1 RNA-binding domain-containing protein | 7.47 | 2.84 | -1.39 | -2.63 | 0.0058 |

| | | | | | | | |
|---|---|---|---|---|---|---|---|
| DVU0904 | recJ | single-stranded-DNA-specific exonuclease RecJ | 13.58 | 5.17 | -1.39 | -2.63 | 0.0024 |
| DVU2538 | thrS | threonyl-tRNA synthetase | 340.59 | 138.11 | -1.30 | -2.47 | 0.0012 |
| DVU0807 | trmU | tRNA (5-methylaminomethyl-2-thiouridylate)-methyltransferase | 29.96 | 2.81 | -3.41 | -10.64 | 0.0003 |
| DVU1079 | trmE | tRNA modification GTPase TrmE | 7.35 | 2.51 | -1.55 | -2.93 | 0.0196 |
| DVU1828 | gidA | tRNA uridine 5-carboxymethylaminomethyl modification protein GidA | 56.17 | 17.69 | -1.67 | -3.18 | 0.0003 |
| DVU0142 | trpS | tryptophanyl-tRNA synthetase | 137.87 | 41.34 | -1.74 | -3.33 | 0.0003 |
| DVU2842 | | type II DNA modification methyltransferase | 119.70 | 57.17 | -1.07 | -2.09 | 0.0018 |
| DVU0953 | tyrS | tyrosyl-tRNA synthetase | 207.39 | 57.07 | -1.86 | -3.63 | 0.0003 |
| DVU0732 | valS | valyl-tRNA synthetase | 76.91 | 30.16 | -1.35 | -2.55 | 0.0003 |

730

731 Table 5. Protein levels measured (pg/cell) per cell in control and FNA treated cells
732 after 2 and 8 h incubation. Protein change detected during the 6 h incubation and the
733 protein change predicted (given average protein half life of 20 h (41)).
734

| | 2 h | 8 h | Amount of protein change over 6 h incubation | Protein change expected due to half life |
|---|---|---|---|---|
| | Protein levels per cell (pg/cell) | | | |
| Control cultures | 2.33±0.35 | 1.97±0.29 | -0.36 | -0.35 |
| FNA-added cultures (4.0 μg N/L) | 2.11±0.18 | 1.55±0.10 | -0.56 | -0.32 |

735
736